Geochemical Journal, Vol. 47, pp. 219 to 234, 2013

Petrology and geochemistry of the back-arc lithospheric mantle beneath eastern Payunia (La Pampa, Argentina): Evidence from Agua Poca peridotite xenoliths

GUSTAVO W. BERTOTTO,[1]* MAURIZIO MAZZUCCHELLI,[2] ALBERTO ZANETTI[3] and RICCARDO VANNUCCI[3,4]

[1]INCITAP. UNLPam-CONICET. Uruguay 151, Santa Rosa (6300), La Pampa, Argentina
[2]Dipartimento di Scienze Chimiche e Geologiche, Università di Modena e Reggio Emilia, P.le S. Eufemia 19, I-41121 Modena, Italy
[3]Istituto di Geoscienze e Georisorse - CNR, U.O.S. di Pavia, Via Ferrata 1, I-27100 Pavia, Italy
[4]Dipartimento di Scienze della Terra, Università di Pavia, Via Ferrata 1, I-27100 Pavia, Italy

(*Received February 5, 2012; Accepted March 13, 2013*)

This paper presents the results of new petrochemical studies carried out on mantle xenoliths hosted in Pleistocene basaltic rocks from the Agua Poca volcano in central-western Argentina. Mantle xenoliths studied are shown to be mainly anhydrous spinel lherzolites with minor amounts of harzburgite and banded pyroxenite, showing highly variable equilibrium temperatures ranging from 820°C to 1030°C at 1.0 to 2.0 GPa. This constitutes evidence that the mantle xenoliths are representative of a large portion of the lithospheric mantle column and that the geothermal gradient is not very elevated as reported in some other Patagonian provinces. Geochemical characteristics of clinopyroxene in the mantle xenoliths allow classification into two groups; Groups 1 and 2. Group 1 contains most of the lherzolites and has light-REE depletion, with slightly positive anomalies of Eu in some samples and extreme Nb and Ta depletion. Group 2 consists of two harzburgitic samples, has flat REE patterns with lower Sm to Lu concentrations, with enriched Sr and negative HFSE anomalies. Based on mineral and residua compositions estimated assuming equilibrium with clinopyroxenes, Group 1 can be considered to be refractory residua after up to 7%, non-modal, near-fractional melting of a spinel-facies Primitive Mantle. Group 2 can be considered to be after *ca*. 13% of partial melting. It is inferred that partial melting events in the lithospheric mantle beneath the Agua Poca occurred in different ages since the Proterozoic, but compared with Group 1, the metasomatic overprint is dominant in Group 2 mantle xenoliths. The calculated melt compositions from Group 2 are interpreted to be transient liquid compositions developed during melt-peridotite interaction, and are different from the host alkaline basalts. The HFSE-depleted composition estimated for the rising melt suggests the presence of a slab-derived component, although the possibility cannot be disregarded (on the basis of present data) that such a geochemical feature is due to segregation of HFSE-bearing minerals during the interaction with the peridotite. Thus, we attribute the metasomatic agent to a basaltic melt and to a minor amount of slab-derived fluids.

Keywords: mantle xenoliths, fractional melting, mantle metasomatism, depleted mantle reservoir, Argentina

INTRODUCTION

Tectonically, southern Argentina, (commonly known as Patagonia), is part of the back-arc region of the East Andean Cordillera, in which Pliocene–Quaternary alkaline basalt-forming volcanic centers are sporadically distributed between 37°S and 53°S. In recent times, more than twenty localities of basalt hosted mantle xenoliths have been reported in the Patagonian region (e.g., Bjerg *et al*., 1994, 1999, 2005, 2009; Varela *et al*., 1997; Gorring and Kay, 2000; Laurora *et al*., 2001; Ntaflos *et al*., 2001, 2007; Kilian and Stern, 2002; Acevedo and Quartino, 2004; Rivalenti *et al*., 2004a, 2004b, 2007a; Conceição *et al*., 2005; Wang *et al*., 2007; Schilling *et al*., 2008; Dantas *et al*., 2009; Scambelluri *et al*., 2009) since the pioneering works of Villar (1975), Niemeyer (1978), Gelós and Hayase (1979), Muñoz (1981), and Labudía *et al*. (1984). Among these localities, only two contain garnet-bearing peridotites; Pali Aike located in southern Patagonia (Skewes and Stern, 1979; Douglas *et al*., 1987; Stern *et al*., 1989; Kempton *et al*., 1999) and Prahuaniyeu, located in northern Patagonia (Ntaflos *et al*., 2001; Bjerg *et al*., 2009; Gervasoni *et al*., 2009). Bjerg *et al*. (2005) suggest that the Patagonian subcontinental lithospheric mantle experienced only minor melt extractions in the garnet peridotite field, while melt extraction was more extensive in the spinel lherzolite field. Furthermore, it was considered that the lithospheric mantle had been moderately to strongly deformed and recrystallized, frequently in the presence of migrating melts (Rivalenti *et*

*Corresponding author (e-mail: gwbertotto@yahoo.com.ar)

al., 2004a; Bjerg *et al*., 2005). Calculation of equilibrium temperatures and pressures indicates an elevated geothermal gradient similar to that of southeast Australia, and an oceanic lithosphere, which led Ntaflos *et al*. (2001, 2003) and Bjerg *et al*. (2005) to propose the presence of rising mantle plume(s) in the back-arc region during the Neogene time.

The mantle xenoliths sampled in Patagonia exhibit geochemical and petrological variations as a function of their distance from the Chilean Trench. Cryptic and modal metasomatism of variable intensity affected the lithospheric mantle in this region (Rivalenti *et al*., 2004a; Bjerg *et al*., 2005). Metasomatic agents recorded in sampled mantle xenoliths vary with distance to the trench and are linked to the presence of subduction components, such as in the localities of Cerro de Los Chenques (Rivalenti *et al*., 2007a) and Cerro del Fraile (Kilian and Stern, 2002; Wang *et al*., 2007). As shown by the recrystallization and growth of newly formed minerals, such as amphibole and phlogopite, the modal metasomatism becomes increasingly noticeable as the distance increases from the trench, and the strongest influence is indicated in Gobernador Gregores xenoliths (Laurora *et al*., 2001; Aliani *et al*., 2004, 2009; Rivalenti *et al*., 2004b). These processes, observed in the distal region, have been attributed to both carbonatitic fluids (Ntaflos *et al*., 1999; Gorring and Kay, 2000) and silicic fluids derived from the subducted plate (Laurora *et al*., 2001; Rivalenti *et al*., 2004b), whereas metasomatism by tholeiitic and alkaline melts has been proposed to have affected a lherzolite–websterite xenolith suite in Cerro de Los Chenques and the Cerro Clark volcanoes (Dantas *et al*., 2009). Metasomatism by silicate melts has been indicated for the mantle xenoliths in the Pali Aike volcanic field (Kempton *et al*., 1999; Stern *et al*., 1999).

In southern Argentina, most of the mantle xenolith localities are distributed south of 40°S parallel; and only three localities with spinel peridotites have been recognized north of the Colorado River (38°S) (Bertotto, 2000, 2002a, 2002b; Jalowitzki *et al*., 2010). In order to understand the compositional variation of the whole lithospheric mantle and its petrologic evolution, more detailed studies of the mantle xenolith are needed in the northern regions. Thus, we focus on the Agua Poca mantle xenolith site, located on the back-arc area of Payunia, La Pampa province, Central-Western Argentina (Fig. 1).

Bertotto (2000) first reported the mantle xenoliths at the Agua Poca volcano as having protogranular and protogranular to porphyroclastic textures. The four mantle xenoliths collected were classified into two types, spinel lherzolite and spinel harzburgite, with textures and whole rock compositions indicative of an upper mantle origin with a minimum provenance depth of 40 km. Subsequently, a detailed geochemical study of the Agua Poca

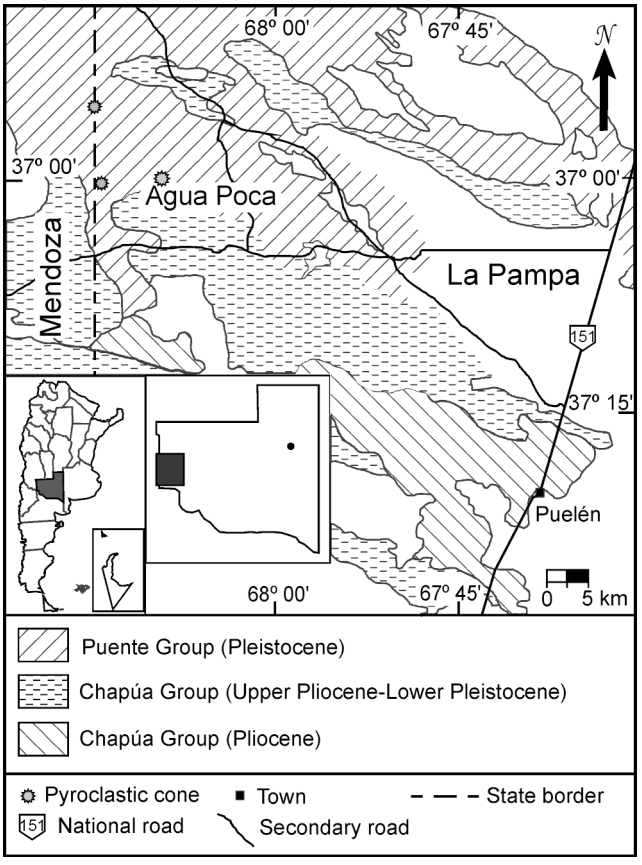

Fig. 1. Location of Agua Poca within the basaltic units of the western La Pampa province.

mantle xenoliths performed by Jalowitzki *et al*. (2010), led to the conclusion that the variability of whole rock composition for the Agua Poca xenoliths might have been caused by varying degrees of partial melting processes in the lithospheric mantle, having either a Depleted Mantle MORB (DMM) or a Primitive Mantle (hereafter PM) with metasomatic enrichment, and involving the interaction of the lithospheric mantle with up to 3% of aqueous fluids derived from a subducted slab. However, whole rock composition does not usually provide full constraints in the case of multi-stage petrologic evolution, particularly when a later metasomatic event caused petrochemical zoning within the samples. Moreover, the whole rock composition of mantle xenoliths can be affected by an interaction with melts and fluids related to the volcanic event that carried them to the surface (e.g., Dantas *et al*., 2009; Kempton *et al*., 1999; Schilling *et al*., 2008; Stern *et al*., 1999). Consequently, such events can hinder the unraveling of the petrochemical processes on the pristine subcontinental lithospheric mantle. To overcome this problem, a mineral micro-analysis investigation is needed, in addition to the detailed petrographic inspection of the

textural relationships, to achieve a comprehensive framework in which to reconstruct the petrologic evolution of the samples.

Here, we present the results of mineral microanalyses for major and trace element compositions obtained from the Agua Poca mantle xenoliths, in order to unravel the petrochemical processes in the underlying pristine lithospheric mantle, and to suggest a petrological model using a combination of results obtained in this study and the whole rock compositions reported in previous literature (Bertotto, 2000, 2003; Jalowitzki *et al*., 2010). We discuss the petrochemical processes that affected the subcontinental mantle beneath the Agua Poca region, and compare such processes with those affecting mantle xenoliths from other Patagonian localities in the abovementioned literature.

Samples of Mantle Xenolith

The mantle xenoliths studied here are hosted in pyroclastic deposits and a lava flow from the Agua Poca volcano. This Pleistocene pyroclastic cone is located in eastern Payunia (37°01′ S, 68°07′ W), in the province of La Pampa, about 530 km east of the Chilean trench (Fig. 1). The host rock is composed of hawaiites, with 7.8 wt.% of MgO, and a trace elements pattern normalized to PM composition (Sun and McDonough, 1989), similar to those of transitional basalts of Stern *et al*. (1990). The magma genesis has been interpreted as the result of low degrees of partial melting of a garnet facies mantle (Bertotto *et al*., 2009).

All the mantle xenoliths are anhydrous spinel peridotites (5 to 20 cm long); the only exception being a composite sample comprising elongated pieces of spinel-bearing pyroxenite. The peridotites are classified as lherzolites (21 samples), and harzburgites (2 samples), (Supplementary Table S1, Fig. 2). The lherzolite textures are Type I porphyroclastic, porphyroclastic to equigranular and protogranular to porphyroclastic (Mercier and Nicolas, 1975) (Figs. 3(a)–(d)). Some lherzolites (AP34C, AP79, AP80, AP87, AP88, AP89, and AP92) show lineation, characterized mainly by the alignment of spinels. The harzburgites (AP15B and AP75) and cpx-poor lherzolites (AP15E and AP15G) exhibit a Type I porphyroclastic and porphyroclastic to equigranular texture (Mercier and Nicolas, 1975). The pyroxenite (AP78) has an equigranular texture and is composed of clinopyroxene-rich bands (AP78-1: plag = 2.3%, opx = 29.7%, cpx = 61.6% and sp = 6.4 modal%), and orthopyroxene-rich bands (AP78-4: opx = 54.5%, cpx = 22.3% and sp = 23.2 modal%). A pyroxenite xenolith also includes the boundary it shared with a host peridotite; the boundary is 5 mm-thick, and its composition is ol = 82.9%, opx = 9.1%, cpx = 5.9% and sp = 2.1 modal%.

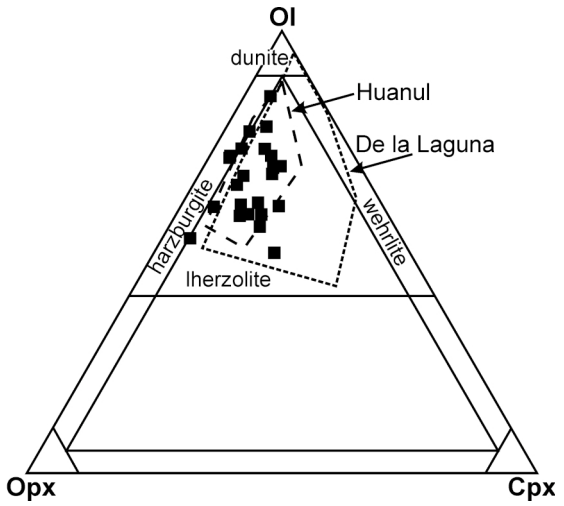

Fig. 2. Modal classification of Agua Poca mantle xenoliths (squares). Also shown (in contours) is the classification of xenoliths from two localities at the same back-arc volcanic zone.

Within the peridotites, olivine occurs mostly as anhedral and subhedral crystals. Olivine generally shows a porphyroclast texture, with dislocation structures (kink bands). The largest olivine reaches up to 6 mm in length and the subhedral grains generally have an average diameter of 0.6 mm (Figs. 3(a)–(c)). The edges of the olivine are mostly ragged and polygonal, and to a lesser extent curved. Olivine crystals in contact with the host basaltic rock are sharply truncated without reaction. Only in small samples (e.g., AP19 and AP75), included in spatter deposits, all the olivines appear dull and are colored black to red under macroscopic observation. In thin section, olivine has isolated and elongated inclusions that become more abundant towards the margin; resembling the oxidized olivine of Johnston and Stout (1984), (Fig. 3(d)).

Orthopyroxene is commonly anhedral and has a maximum length of 11 mm (Figs. 3(a) and (b)). Similarly to olivine, orthopyroxene has a margin that is mostly ragged and polygonal, and to a lesser extent, curved. The porphyroclastic orthopyroxene commonly has exsolution lamellae of clinopyroxene. Orthopyroxene in two peridotite samples (AP85 and AP88) shows reaction textures, where it makes contact with the host basaltic rock.

Clinopyroxene has a variable modal content ranging from 4.0 to 22.5%. The most cpx-depleted peridotites are: AP15B, AP75, AP15E and AP15G (*ca*. 4–5 modal% of cpx), while the most cpx-enriched lherzolite is AP89 (22.5 modal% of cpx), (see Table S1). Clinopyroxene is anhedral and has a maximum size of *ca*. 2 mm. The reaction rim is frequently observed, although it is weak and rarely shows a complete development of recrystallized corona. Clinopyroxene commonly has a submicroscopic exsolution lamellae texture, as well as melt/fluid inclu-

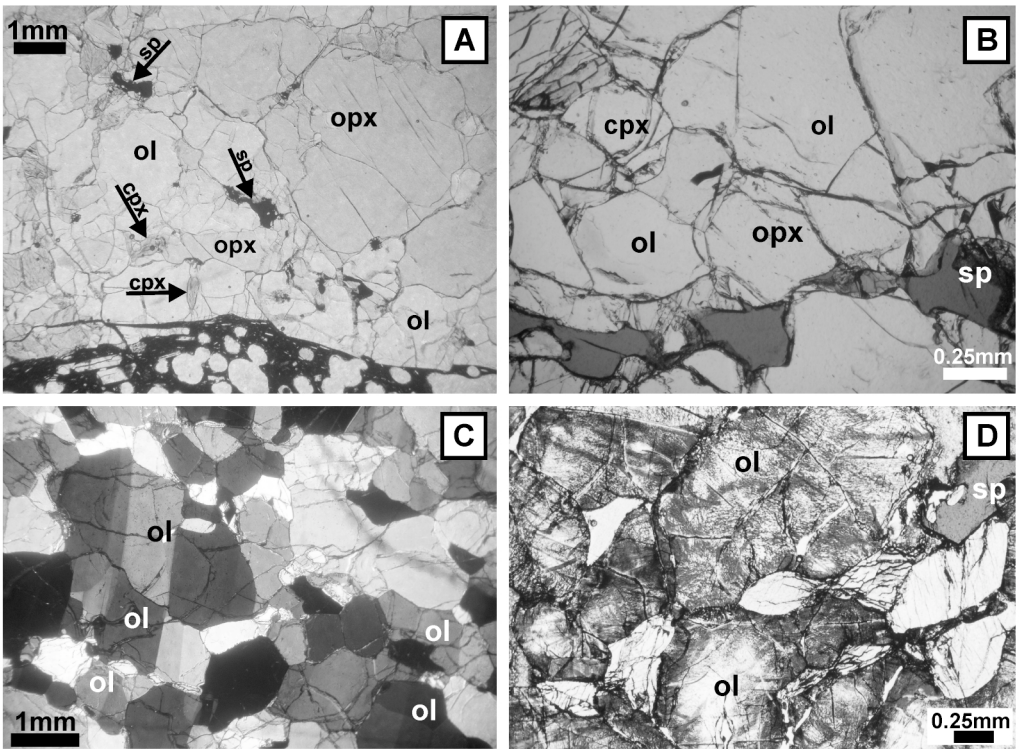

Fig. 3. Photographs of thin microscope sections of Agua Poca mantle xenoliths. (a) Porphyroclastic texture in harzburgite with orthopyroxene (opx), olivine (ol), clinopyroxene (cpx) and spinel (sp). Note unaltered sharp contact with basalt, PPL. (b) Porphyroclastic texture in lherzolite with orthopyroxene (opx), olivine (ol), clinopyroxene (cpx) and spinel (sp). Note spinel shape, PPL. (c) Lherzolite, with kink-banded olivines (ol), XPL. (d) Lherzolite with exsolutions developed by olivines. Note that exsolutions are marked in the margins and decrease towards the crystal cores, and that the only affected mineral is olivine, PPL.

sions. The inclusions are particularly dominant in samples AP2-1, AP15B, AP15E, AP15G, and AP88.

Spinel is 0.1 to 0.4 mm in size, and occupies between 1 and 5% in modal composition. The shape is anhedral to subhedral (Figs. 3(a), (b) and (d)). Holly-leaf shaped spinel, (Mercier and Nicolas, 1975), is commonly observed in porphyroclastic samples (Fig. 3(b)).

Glass veinlets with a maximum thickness of 10 μm are observed in several samples (e.g., AP75, AP80, AP91B) using the scanning electronic microscope. These glass veinlets are directly in contact with olivine and occur as an interstitial phase in the spongy rims of clinopyroxene and develop minute crystals of Cr-rich spinel against the primary spinel.

Microanalytical Methods

Major elemental analyses of olivine, orthopyroxene, clinopyroxne, and spinel were carried out at the "Dipartimento di Scienze della Terra, Università di Modena e Reggio Emilia," Italy, with an ARL-SEMQ electron microprobe in wavelength dispersive mode, (with an accelerating potential of 15 kV, a beam current of 20 nA, spot size of 4–7 μm and counts of 4 s for background and 20 s for peaks). Natural minerals and metallic Ni were used as standards. Counts were converted to weight percent oxides using the PROBE software developed by J. J. Donovan (Advanced Microbeam, USA). Results are considered to be accurate within 2–6%.

Trace element compositions of two pyroxenes were analyzed by laser-ablation (LA)-ICP-MS at the "CNR-Istituto di Geoscienze e Georisorse, Sezione di Pavia." The LA ICP-MS is a double focusing sector field analyzer, (Finnigan MAT Element), coupled with a Q-switched Nd:YAG laser source (Quantel Brilliant); the fundamental emission of which is in the near-IR region (1064 nm) and is converted to 266 nm by two harmonic generators. Helium was used as the carrier gas, mixed with Ar downstream of the ablation cell. The spot diameter was varied in the range of 30–100 μm. A BCR2-g reference sample was used for calibration with ^{44}Ca, as an internal standard for clinopyroxene and ^{29}Si, for orthopyroxene. Precision and accuracy, obtained by analyses of NIST SRM612 reference standard, were better than 10% for concentrations at the ppm level. Detection limits were typically in the range of 100–500 ppb for Sc; 10–100 ppb for Sr, Zr,

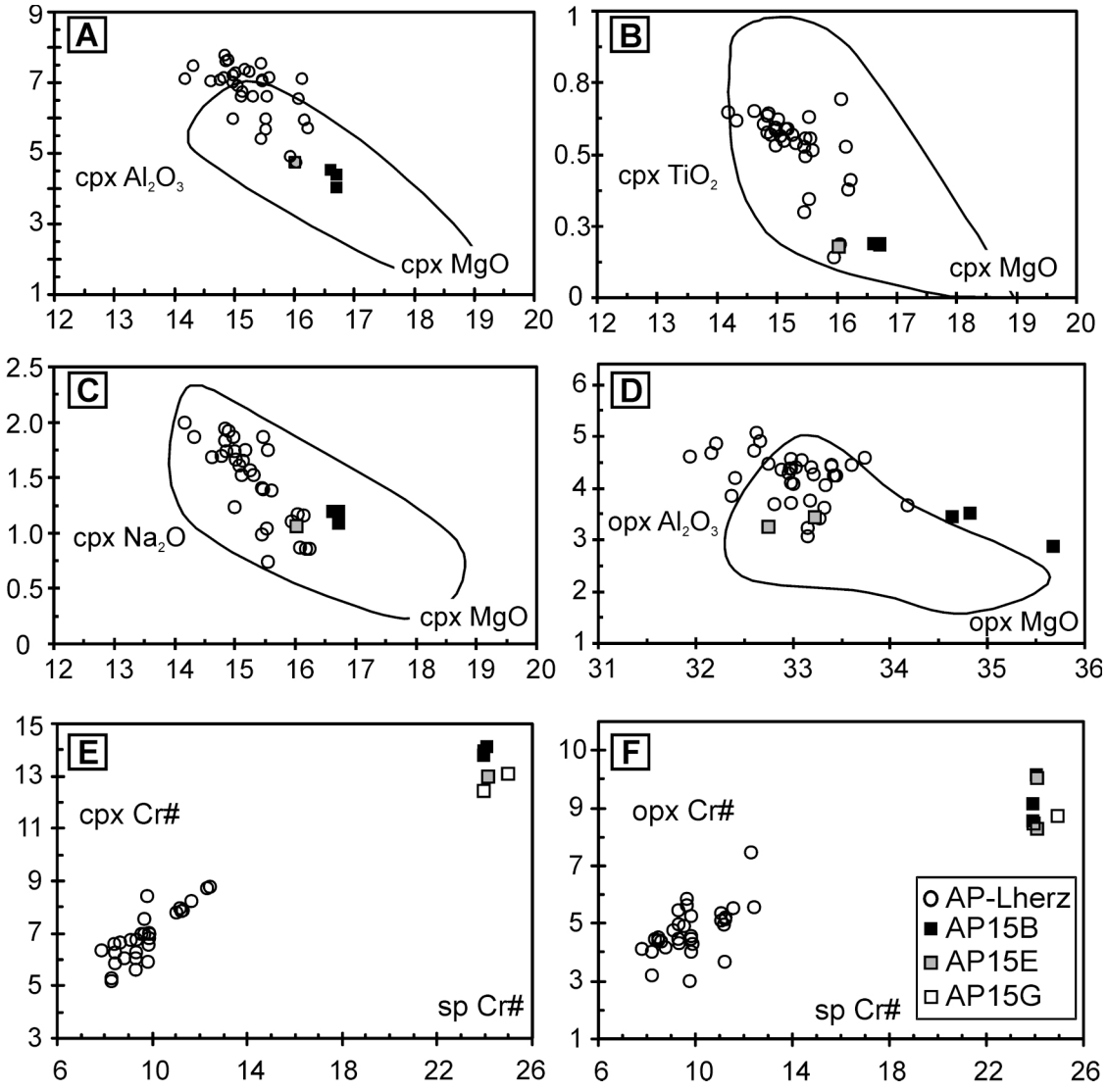

Fig. 4. Major element (wt.%) variation trends in clinopyroxene (A–C, Al_2O_3, TiO_2 and Na_2O vs. MgO), and orthopyroxene (D, Al_2O_3 vs. MgO). Fields of clinopyroxenes and orhopyroxenes of anhydrous peridotites from Patagonia are displayed for comparison (Rivalenti et al., 2004a; Bjerg et al., 2005; Ntaflos et al., 2007). Clinopyroxene and orthopyroxene Cr# vs. spinel Cr# (E and F). Samples with highest Cr# are those with low modal % of clinopyroxene and signs of metasomatism (AP15B, AP15E and AP15G).

Ba and Gd; 1–10 ppb for Y, Nb, La, Ce, Nd, Sm, Eu, Dy, Er, Yb, Hf, and Ta; and usually <1 ppb for Pr, Th, and U.

RESULTS

Major element composition of minerals

Results of mineral microprobe analyses for the peridotite xenoliths are shown in Supplementary Table S2. Olivine in lherzolite has a forsterite content in the range of 88.2–90.9 mol%. The highest value in all the mantle xenoliths analyzed in this study is found in the cpx-poor lherzolite AP51G, and the lowest value is obtained from the olivines, from the lherzolite in the composite sample AP78-3. Clinopyroxene in all samples is diopside, with $En_{47–52}$, $Fs_{2–5}$, and $Wo_{45–49}$. The Mg# [100Mg/(Mg + Fe_{tot}) molecular ratio] varies between 88.7 and 91.7. Al_2O_3, TiO_2, and Na_2O decrease, and CaO increases with an increase of MgO (Figs. 4(a)–(c)). Variations in amounts of TiO_2, Na_2O, and CaO, are within the range of Patagonian anhydrous xenoliths (Rivalenti *et al.*, 2004a; Bjerg *et al.*, 2005; Ntaflos *et al.*, 2007), however, the compositional field of Al_2O_3 extends towards higher values. Orthopyroxene is enstatite in all samples, with $En_{86–90}$, $Fs_{9–12}$, and $Wo_{0.6–1.8}$. Al_2O_3 decreases with in-

Table 1. Representative LAM ICP-MS analyzes of clinopyroxene and orthopyroxene

Sample	AP2-1	AP15B	AP15E	AP34A	AP78-3	AP80	AP88	AP91B	AP91D
clinopyroxene									
Rb (ppm)	0.069	0.032	0.101	0.062	0.026		0.327	0.052	0.041
Ba	0.475	0.168	0.110		0.424	0.286	0.154	0.211	0.626
Th	0.020	0.012	0.016	0.013	0.008	0.003			0.038
Nb	0.146	0.055	0.045	0.035	0.125	0.015	0.094	0.038	0.060
Ta	0.017	0.009	0.013	0.007	0.013	0.007	0.002	0.009	
La	0.203	0.875	0.733	0.232	0.446	0.140	0.081	0.985	0.192
Ce	1.620	2.987	2.918	1.788	1.574	1.351	0.740	4.818	1.428
Pr	0.414	0.458	0.425	0.513	0.261	0.437	0.247	0.979	0.375
Sr	42.573	44.297	41.698	33.990	55.117	24.465	10.953	50.760	19.258
Nd	3.210	2.410	2.460	3.120	1.489	3.208	2.165	5.455	2.507
Sm	1.533	0.874	0.735	1.429	0.625	1.778	1.152	2.260	1.413
Zr	15.45	11.81	10.43	19.50	10.45	18.60	12.94	27.40	14.55
Hf	0.771	0.343	0.303	0.733	0.394	0.774	0.662	0.973	0.624
Eu	0.720	0.286	0.291	0.654	0.305	0.697	0.542	0.918	0.652
Gd	1.747	0.796	0.759	2.027	0.833	2.448	1.778	2.633	1.657
Tb	0.393	0.136	0.149	0.394	0.164	0.462	0.378	0.465	0.335
Dy	2.697	0.857	1.137	2.710	1.103	2.928	2.570	3.023	2.435
Y	13.933	6.133	5.980	15.813	6.427	16.973	13.900	17.248	13.173
Er	1.657	0.562	0.725	1.594	0.662	1.965	1.558	1.815	1.383
Yb	1.677	0.594	0.729	1.797	0.564	2.023	1.468	1.637	1.492
Lu	0.205	0.077	0.094	0.235	0.093	0.281	0.205	0.250	0.204
Sc	50.447	53.817	54.578	59.367	38.307	57.853	51.273	55.563	53.823
orthopyroxene									
Rb		0.133	0.020			0.029	0.035	0.024	
Ba									0.131
Th	0.008	0.018	0.015		0.009	0.006		0.004	0.004
Nb	0.010	0.019		0.014	0.041				
Ta							0.016	0.011	
La				0.013	0.033	0.005		0.015	0.011
Ce	0.032	0.049	0.243	0.025		0.012		0.037	
Pr	0.008	0.007	0.009	0.006		0.011	0.016		
Sr	0.141	0.076	0.094	0.182	0.053	0.096	0.029	0.228	0.050
Nd				0.051				0.085	0.043
Sm	0.085	0.056	0.044	0.047		0.061		0.034	
Zr	1.146	0.676	0.587	0.846	0.668	1.159	0.977	1.900	0.760
Hf	0.078	0.061		0.061		0.053		0.082	0.105
Eu			0.040	0.019	0.023	0.034		0.024	
Gd		0.093		0.050	0.078		0.185	0.055	0.041
Tb	0.047			0.008	0.012	0.026		0.012	0.018
Dy	0.188	0.072	0.054	0.079		0.142	0.190	0.159	0.158
Y	1.288	0.462	0.451	0.801	0.487	1.150	1.187	1.140	0.825
Er	0.141	0.130	0.138	0.159	0.108	0.144		0.135	0.103
Yb	0.338	0.126	0.130	0.272	0.099	0.330	0.389	0.332	0.250
Lu	0.046	0.015	0.029	0.017	0.020	0.049	0.074	0.056	0.048
Sc	19.485	14.670	16.910	15.020	11.040	17.000	16.920	17.665	14.700

Blank values, below detection limit.

creasing MgO (Fig. 4(d)), and TiO_2 shows a similar weak negative correlation against MgO. Spinel in all samples has Mg# ranging from 75.5 (AP15E) to 85.3 (AP80), while Cr# [100Cr/(Cr + Al) molecular ratio] varies from 7.8 (AP89) to 24.9 (AP15G), (Figs. 4(e) and (f)). Spinel from samples AP15B, AP15E, and AP15G has markedly higher Cr# values than that in the rest of the Agua Poca samples.

Because of the small size of the sub-microscopic glass veinlets, only two microprobe analyses could be achieved on sample AP91B. The glass composition (average of two similar analyses) is a silicate melt, with 46.9 wt.% SiO_2, 25.5 wt.% Al_2O_3, 12.2 wt.% CaO, 9.2 wt.% MgO, 3.1 wt.% FeO_t, 2.2 wt.% Na_2O, 0.1 wt.% K_2O; showing a high percentage of Al_2O_3 and CaO in comparison with that of the host basaltic rock.

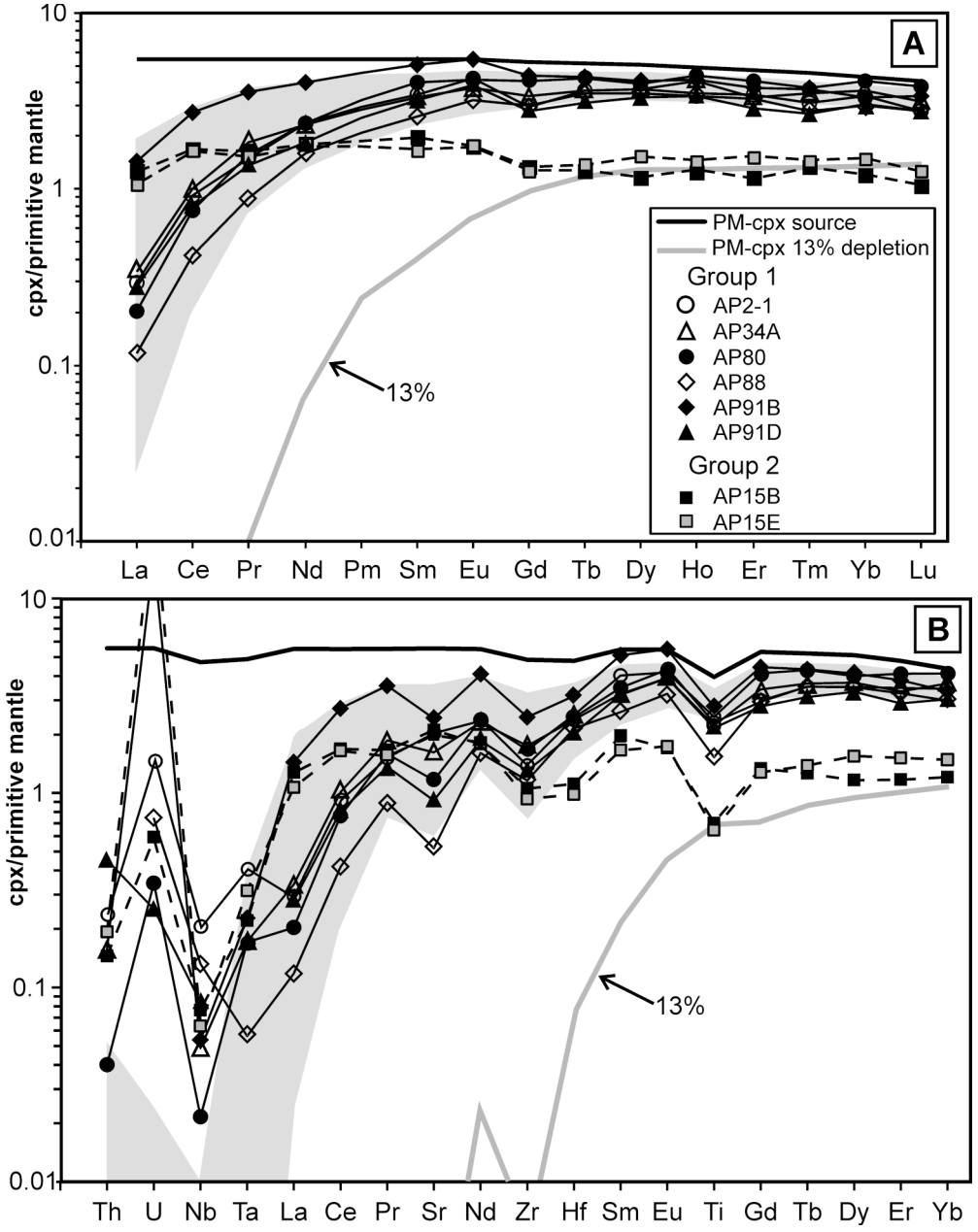

Fig. 5. Primitive Mantle-normalized (Sun and McDonough, 1989) patterns of Agua Poca clinopyroxenes. Gray area represents melt-depletion patterns of a clinopyroxene from the Primitive Mantle (Sun and McDonough, 1989) which has suffered from 1 to 5% non-modal fractional melting. Solid gray line represents 13% melt-depletion pattern. Parameters of calculus are indicated in the text.

Trace element composition for clino- and orthopyroxenes

Trace element compositions of clinopyroxene and orthopyroxene in the peridotite samples are shown in Table 1.

The characteristics of rare earth element (REE) patterns normalized to PM value in clinopyroxene, (Sun and McDonough, 1989), allowed us to distinguish two groups of samples: Group 1 and Group 2 (Fig. 5(a)). Group 1 has light (L)-REE depletion patterns [0.04 to 0.4 in La_N/Yb_N; ~3–5 in heavy (H)-REE_N], with slightly positive anomalies of Eu in some samples. Group 1 has extreme Nb and Ta depletion on the spidergram, while U and Th concentrations are variable (Fig. 5(b)). Slightly negative Sr, Zr, Hf, and Ti anomalies on the spidergram, are also recognized in Group 1. The overall characteristics of the Group 1 clinopyroxenes are similar to those recognized

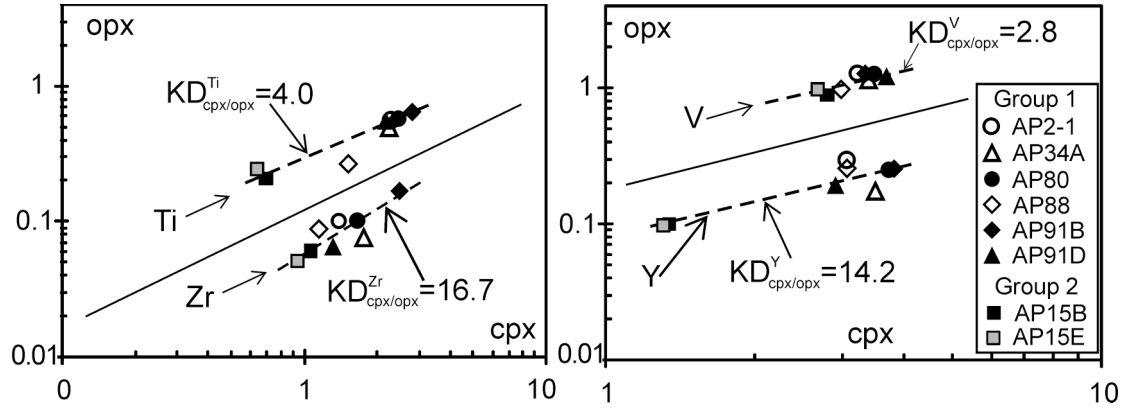

Fig. 6. Correlations of selected trace elements between orthopyroxene and clinopyroxene, KD values were calculated by averaging all analyzes plotted for each element.

in worldwide Depleted Mantle reservoirs of the subcontinental mantle, as noted in Cerro de los Chenques (Patagonia; Rivalenti *et al*., 2007a), north-eastern Brazil (Rivalenti *et al*., 2007b), and the Italian Western Alps (Mazzucchelli *et al*., 2010). Compared to Group 1, Group 2 has flat REE patterns with lower Sm to Lu concentrations (0.7 to 1.1 in La_N/Yb_N; with a maximum of up to a value of 2 in middle, (M)-REE_N) (Fig. 5(a)). Group 2 has no noticeable L-REE depletion pattern (which is seen in Group 1). Group 2 also has negative Zr, Hf, and Ti anomalies and a positive Sr anomaly on the spidergram. Extreme Ta and Nb depletion on the spidergram, as well as variable U and Th concentrations, are also recognized in Group 2 (Fig. 5(b)). The characteristics of Group 2 clinopyroxenes resemble those found in mantle xenoliths from some localities in the Patagonian province (e.g., Cerro de los Chenques; Rivalenti *et al*., 2007a), as well as from other worldwide localities (e.g., Xu *et al*., 1998; Ozawa, 2001), and are considered to belong to a lithospheric mantle deeply modified by the percolation of large volumes of external melt.

Due to extremely low concentrations, it is difficult to handle the orthopyroxene for trace element compositional analysis. However, it was possible to see that some of the trace elements are present in relatively higher concentrations (e.g., Sc, Ti, V, Y, and Zr) (see Table 1).

The results of the above elemental compositions are used to mainly assess the orthopyroxene–clinopyroxene chemical equilibrium. Figure 6 shows the positive correlations of Ti, Y, V, and Zr concentrations between orthopyroxene and clinopyroxene. The apparent cpx/opx partition coefficients ($KD_{cpx/opx}$), as shown in Fig. 6, are in the range of those calculated using the $^{cpx/L}D$ and $^{opx/L}D$ values of Ionov *et al*. (2002), and Adam and Green (2006). This result indicates that the clinopyroxenes are in equilibrium with the orthopyroxenes in the mantle xenoliths, at least, in the above elemental compositions.

Whole rock composition of the mantle xenoliths

Bertotto (2000, 2003) reported the whole rock composition of the same Agua Poca mantle xenoliths studied here. The data set is compiled in Supplementary Table S3. Amounts of MgO in the mantle xenoliths range between 38 and 43 wt.%. The compositional variations of MgO are within the range of those reported by Jalowitzki *et al*. (2010), and show a negative correlation with Al_2O_3, CaO, TiO_2, and Na_2O content (Fig. 7). As a whole, the Agua Poca mantle xenoliths are, on average, more fertile than the spinel facies from Patagonian localities (Rivalenti *et al*., 2004a; Bjerg *et al*., 2005, Ntaflos *et al*., 2007), expanding the compositional fields towards a lower MgO content and higher TiO_2, Na_2O, CaO and Al_2O_3 values.

The REE pattern and spidergram for the whole rocks normalized to PM composition are shown in Figs. 8(a) and (b). Unaltered samples (AP34A, AP80 and AP91B), have a pattern depleted in L-REE. Within the (M)- to H-REE region, the REE pattern becomes flat with a slight positive slope. The sample AP91B has a similar M- to H-REE concentration as those of the PM value. Sample AP19, with altered olivine, shows a less-depleted L-REE pattern than those in the other samples. Among all the analyzed samples, La/Yb_N ratios range from 0.13 (AP80), to 0.53 (AP19). The spidergram is characterized by no Ti and Sr anomalies (or slight to modest anomalies). All the samples indicate a positive Zr anomaly, which is associated with positive Nb and Hf anomalies in samples AP19 and AP34A.

Discussion and Conclusion

Geothermal gradient of the lithospheric mantle

The equilibrium temperatures of the Agua Poca peridotite xenoliths, estimated from major element contents in clinopyroxene and orthopyroxene cores, are shown in Supplementary Table S4. Equilibrium tempera-

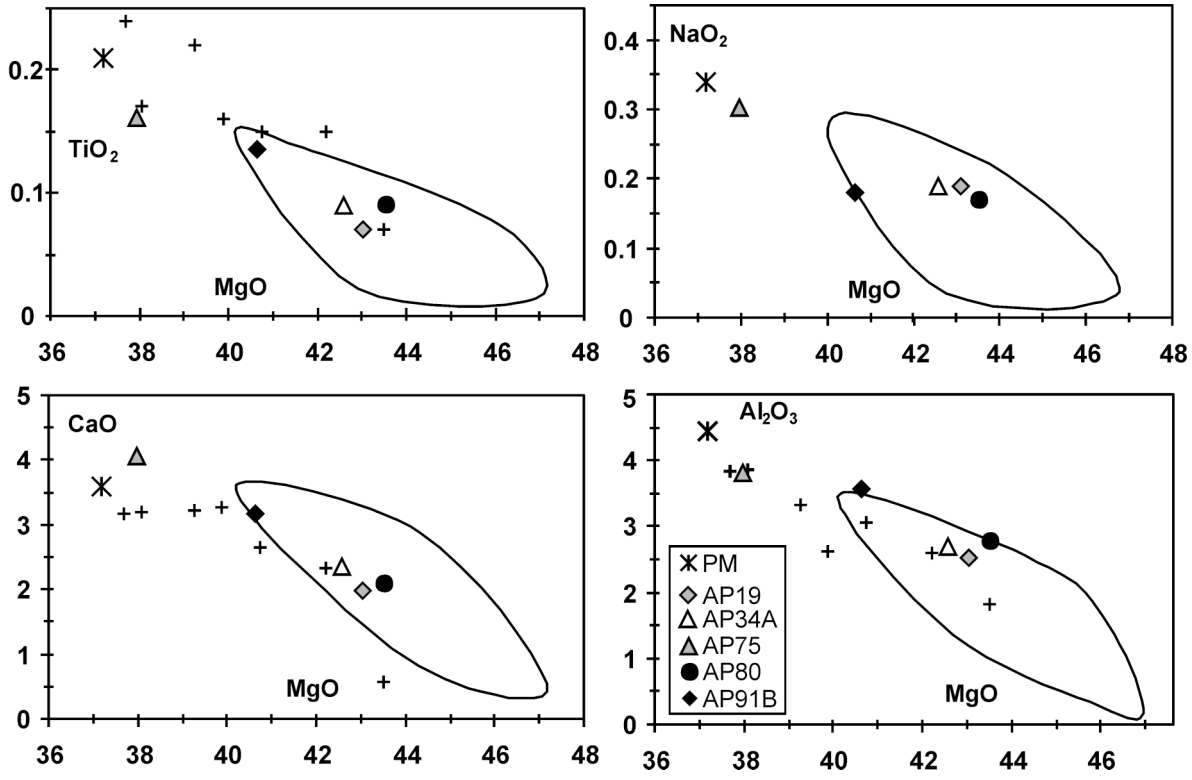

Fig. 7. Major oxides variation of Agua Poca mantle xenoliths (whole rock). Primitive Mantle compositions (McDonough, 1990) are illustrated with a comparison of the field of variation of anhydrous peridotites from Patagonia (Rivalenti et al., 2004a; Bjerg et al., 2005), and Agua Poca xenoliths suite of Jalowitzki et al. (2010) (crosses).

tures calculated with the two-pyroxene thermometer of Brey and Köhler (1990), range from 843°C to 1080°C (at 1.5 GPa). Compared with previous estimations of equilibrium temperature for mantle xenoliths from Patagonia using a two-pyroxene geothermometer (Rivalenti *et al*., 2004a; Bjerg *et al*., 2005; Ntaflos *et al*., 2007), the Agua Poca peridotite xenoliths show lower temperatures than those of spinel-facies peridotites from Prahuaniyeu, Laguna Fría, and Traful in North Patagonia, and Tres Lagos and Pali Aike in South Patagonia, but show temperatures similar to those of Cerro del Mojón-Comallo in North Patagonia, and at Fraile-Las Cumbres in South Patagonia.

Equilibrium temperatures estimated according to Taylor (1998) vary from 772°C to 1034°C and show a strong correlation with those of Brey and Köhler (1990). The temperature estimation provided by the Ca-opx thermometers of Brey and Köhler (1990) and Nimis and Grütter (2010) is in the range of 809–1007°C. The lowest temperature was obtained from lherzolite AP92 (772–855°C), and the highest temperature was obtained from lherzolite AP2-1 (995–1080°C). Thus, the Agua Poca peridotite xenoliths document a temperature variation of the mantle column of around 200°C. Equilibrium temperatures obtained using the two-pyroxene geothermometers, are strongly correlated with the pressure calculated using the empirical geobarometer of Mercier (1980), which varies from 1.0–1.1 GPa (AP92, AP91D) to 1.9–2.0 GPa (AP2-1, AP88, AP15B, AP15G, AP15E). This indicates that the peridotite xenoliths may have been derived from a mantle section *ca*. 30–70 km deep. Moreover, from the above *P–T* condition, the geothermal model gradient is calculated to be *ca*. 8–11°C/km and this is similar to that of Bjerg *et al*. (2005), who suggested that it could be caused by Neogene–Quaternary back-arc volcanism.

Evidence and estimated degree of partial melting of the lithospheric mantle

Bertotto (2003) pointed out that the variation of the cpx/opx vs. cpx modal content in the peridotite xenoliths of Agua Poca matches that predicted from a model of partial melting. More detailed geochemical data of the peridotite xenoliths obtained in this study also indicate that several petrochemical features are consistent with a derivation of residue, which is the result of a melt extraction by variable degrees of partial melting. For instance, a focus on the major element compositional correlation

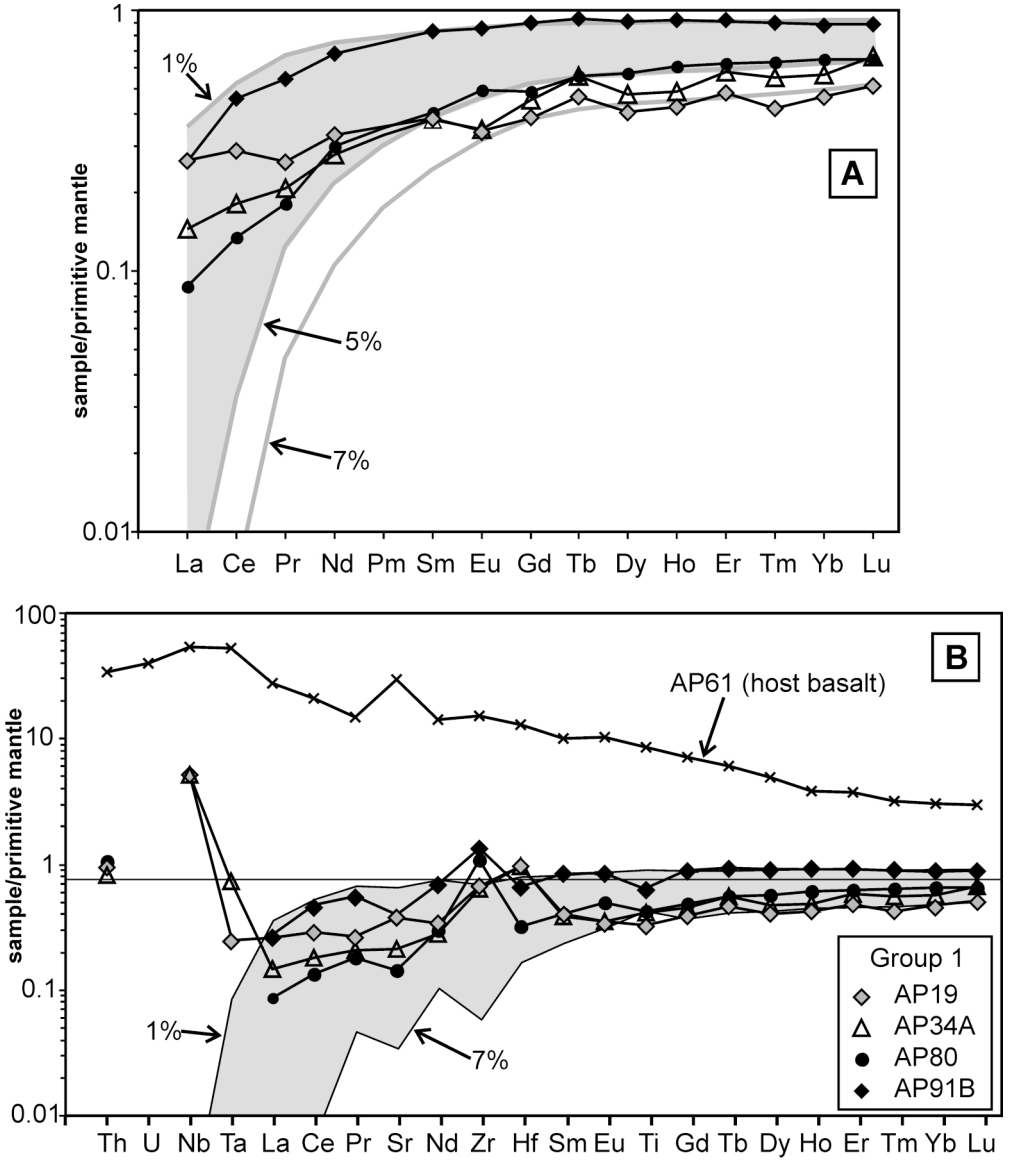

Fig. 8. (a) Primitive Mantle-normalized (Sun and McDonough, 1989) REE patterns of whole rock compositions of the Agua Poca mantle xenoliths. Gray area represents depletion patterns of a Primitive Mantle which suffered from 1 to 5% non-modal fractional melting. Also indicated is a pattern of 7% depletion. (b) Primitive Mantle-normalized (Sun and McDonough, 1989) extended trace elements patterns of whole rock Agua Poca mantle xenoliths, and host basalt (AP61). Gray area represents depletion patterns of a Primitive Mantle which suffered from 1 to 7% non-modal fractional melting. Parameters of calculus are indicated in the text.

among five peridotite xenoliths, (AP91B, AP19, AP34A, AP80, and AP15E (from Jalowitzki *et al*., 2010)), have whole rock Al_2O_3 contents decreasing from 3.6 wt.% to 1.8 wt.%, which is well correlated with the decrease of Al_2O_3 in the clinopyroxenes, and with the increase of forsterite contents in the olivine (ranging from 89.4 to 90.5). Moreover, the value of spinel-Cr# from the five samples ranges from 8.2 to 24.1, and the Mg# value in the orthopyroxene varies between 89.7 and 91.0, which is in accord with variations in whole rock, clinopyroxene, and olivine compositions.

In order to estimate how the degree of partial melting has affected the Agua Poca peridotite xenoliths, whole rock geochemical features are compared to those calculated for residua, assuming a non-modal fractional melting of a spinel-facies peridotite with PM composition. This calculation was performed using three parameters: 1) the mantle source modal composition from Johnson *et*

al. (1990); 2) the melting mode from Gaetani and Grove (1998); and 3) the solid-melt partition coefficients from Ionov *et al*. (2002). The REE pattern for AP80 generally corresponds to that of the residua after a 5% melt extraction, but La to Nd becomes more enriched than in the calculated residue (Fig. 8(a)). The degree of partial melting (calculated using the equation from Batanova *et al*. (1998)), from the Al_2O_3 composition of the associated spinels, (see Table S2), was 3–4%, which seems to be slightly unmatched in both the calculations. The REE patterns for AP19, AP34A and AP91B, correspond well to those of the residue after a 1–7% extraction of melts. The degree of melt extraction calculated, based on the spinel compositions, was 1–7%, which almost matches the former calculations. However, the enrichments in L-REE and other highly incompatible elements for the samples AP19 and AP34A do not match the calculated values, because the residue is significantly depleted in highly incompatible elements by partial melting (Figs. 8(a) and (b)). A strong interaction with the host basaltic rock was dominantly observed in sample AP19. This effect may have disturbed the precise estimation of the degree of melt depletion on the basis of whole rock compositions.

To eliminate the influence of alteration, we focused on the geochemical signature of clinopyroxene. The trace element compositions of Group 1 clinopyroxenes, (i.e., lherzolites AP2-1, AP34A, AP80, AP88, AP91B and AP91D), correspond to the refractory residua after ~1–5% non-modal fractional melting of spinel-bearing peridotite with PM composition (Fig. 5(a)), except only partly for Th, U, and Nb. Group 2 clinopyroxenes in samples AP15E (cpx-poor lherzolite) and AP15B (harzburgite) show that Gd–Lu signatures in the REE pattern are compatible to those which underwent approximately 13% depletion by non-modal fractional melting of the PM source (Fig. 5(a)). The estimated degree of depletion is also consistent with the degree of melt extraction on the basis of spinel composition. Melt extraction degrees estimated from Al-rich spinels included in most of the Agua Poca lherzolite xenoliths coexist with Group 1 clinopyroxene (i.e., in 16 samples) and are estimated to range from 1 to 5.5%, whereas more refractory spinel compositions from cpx-poor lherzolite and harzburgite in the Group 2 clinopyroxenes (AP15B, E, and perhaps, AP15G), suggest a larger degree of partial melting (*ca*. 12%). These results are strictly consistent with the degrees of melt extraction estimated on the basis of REE content of clinopyroxene. However, the L- to M-REEs and the other highly incompatible elements (e.g., Sr, Zr, and Hf) are significantly enriched of the depletion of PM residue (Figs. 5(a) and (b)), suggesting a significant metasomatic overprint in the two samples, as mentioned in detail below.

Timing of partial melting of the lithospheric mantle

The Re–Os isotope and its model age for the mantle xenolith provide a tool for deducing both the development of the lithospheric mantle and the timing of the latest major melt extraction. Schilling *et al*. (2008) demonstrated the ages of the Re–Os model and provided estimations of minimum depletion ages for four samples of Agua Poca xenoliths (AP15, AP78-Z2, AP80, and AP91B). Of these four samples, AP15, AP80, and AP91B are the same samples as studied here and are classified as Groups 1 and 2 for clinopyroxene. Except for AP78-Z2 showing unreal future age, the three model ages yielded 0.33 Ga for AP91B, 0.89 Ga for AP80, and 1.6 Ga for AP15, which are the best estimations for the timing of melting events recorded in each Agua Poca mantle xenolith. Moreover, AP80 was determined to have a high $^{143}Nd/^{144}Nd$ ratio and to be a Proterozoic Nd-isotope model (Conceição *et al*., 2005).

Schilling *et al*. (2008) pointed out the occurrence of a negative correlation between forsterite olivine contents with $^{187}Os/^{188}Os$ ratios, as well as a remarkably good correlation for the Al_2O_3 versus $^{187}Os/^{188}Os$ diagram in the Agua Poca mantle xenoliths, which led to a proposed depletion age of 2.14 Ga. This age approaches the estimated model age of 2 Ga, which is interpreted as the formation of the subcontinental mantle-continental crust assemblage in the region of Central Chile (33°S) by Montecinos *et al*. (2008), based on the Hf isotope analyzes on zircons. Schilling *et al*. (2008) concluded that the Agua Poca mantle xenoliths might be relicts from the lithospheric mantle of the Cuyania terrane, which were formed probably as part of the Laurentia continent during the Proterozoic.

Metasomatism of the lithospheric mantle

The Agua Poca mantle xenoliths studied here show a more or less metasomatic overprint signature in both whole rock and clinopyroxene compositions. In particular, most refractory samples have harzburgitic modal and Group 2 clinopyroxene compositions, i.e., AP15B and AP15E, display significant enrichment with gradually increasing from Eu to Th in spidergrams. The geochemical trend calculated by the partial melting model, indicates that the two harzburgitic samples are subjected to a higher degree of partial melting (*ca*. 13%), than those of the spinel lherzolite (*ca*. 1–7%), on the basis of the HREE concentrations (Figs. 5 and 8). However, in this case, the enrichment signature should be dominant in the two rare refractory samples, and not in the common spinel lherzolite. The metasomatic agents which have high Eu to Th concentrations, particularly in U, are thought to have occurred by two processes and the metasomatic overprint is related to either: i) a continuous influx of melt (or fluid) during an *in-situ* partial melting event in the initial

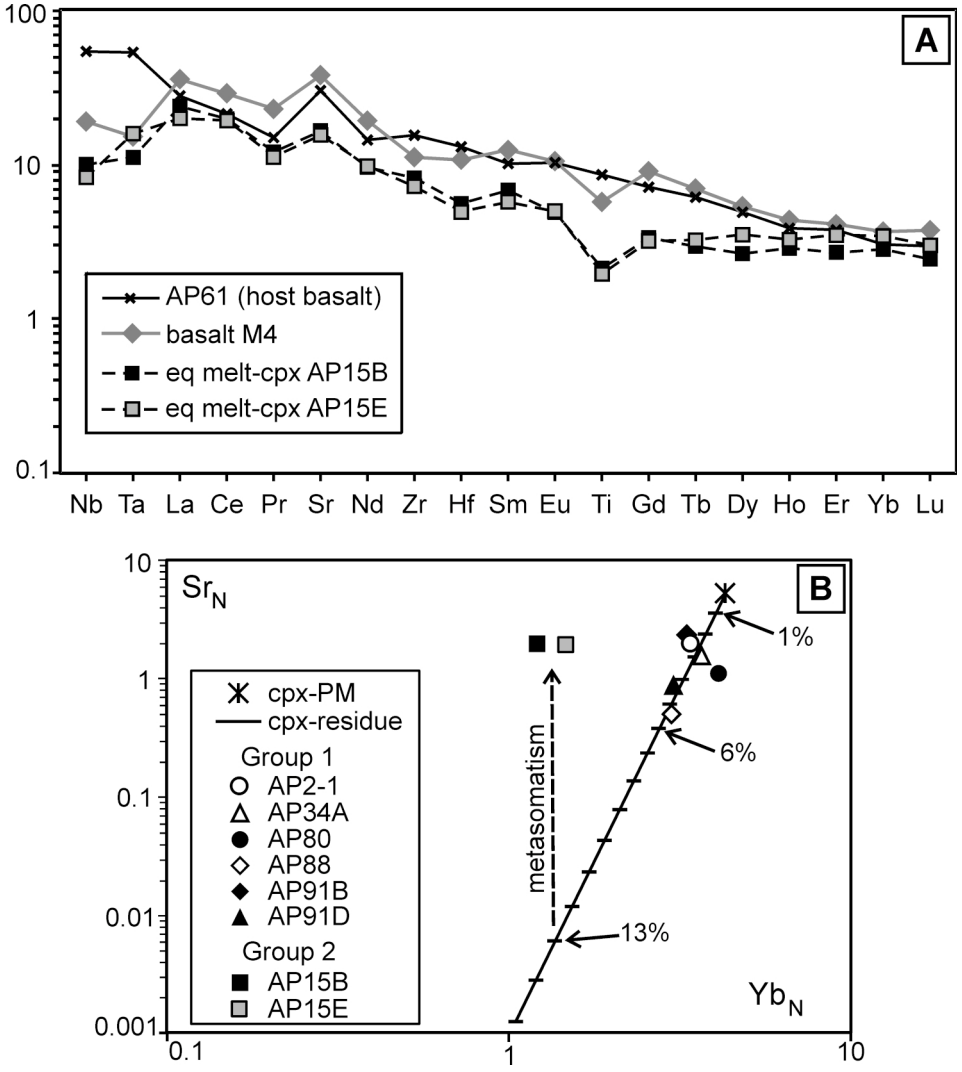

Fig. 9. (a) Potential melts in equilibrium with clinopyroxenes AP15B and AP15E, compared with host basalt (AP61), and basalt (M4) from same volcanic field with signs of slab contamination (e.g., Nb–Ta negative anomaly). Equilibrium melts calculated with partition coefficients from Ionov et al. (2002). Data of basalt (M4) from Bertotto et al. (2009). (b) Sr_N vs. Yb_N diagram of Agua Poca clinopyroxenes. Solid black line represents melt-depletion trend from 1 to 15% of a clinopyroxene from the Primitive Mantle (Sun and McDonough, 1989); black horizontal lines indicate a 1% depletion increment. Note that samples AP15B and AP15E are clearly separated from the melting trend, possibly due to the metasomatic enrichment of Sr (dashed line). Parameters of calculus are the same as Fig. 5 and are indicated in the text; values normalized to Primitive Mantle of Sun and McDonough (1989).

lithospheric mantle, (e.g., the "Open System Melting" proposed by Ozawa and Shimizu (1995) and Ozawa (2001) and also numerically simulated by Vernières *et al.* (1997)) or ii) an influx of new melt into ancient depleted lithospheric mantle, produced by the late magmatism. The REE pattern in some of the clinopyroxenes from the Miyamori harzburgite shown in Ozawa (2001) bear a good resemblance to those of our Group 2, and this suggests that clinopyroxene may support the first model. Following the Open System Melting model, the best fit was obtained from the interaction of a melt/fluid with a composition similar to a melt in equilibrium with hornblende (Ozawa, 2001). The estimated degree of melting, and the trapped melt fraction, were calculated to be 22% and 2.4%, respectively.

In order to test the influx of new melt into ancient depleted lithospheric mantle, we assumed that the chemical equilibrium with migrating melts occurred without subsolidus redistribution, and/or volumes of trapped melt. The potential melts in equilibrium with the clinopyroxenes

of Group 2, were inferred to have low Nb and Ta, high La/Yb, a positive Sr anomaly, and a negative Ti anomaly (Fig. 9(a)). Indeed, the relative depletion of HFSE in the estimated melts could have resulted from the segregation of HFSE-favor accessory minerals during the melt-peridotite interaction (see Rivalenti *et al*., 2007a and references therein). However, the geochemical features of the obtained melt are usually considered as representative of slab-derived components. In particular, Nb and Ta concentrations in the estimated melt, having a higher incompatibility in an anhydrous silicate melt, lack enrichment, and have low Ti concentrations. This signature is consistent with the proposal of Klimm *et al*. (2008), who suggest that the temperature in the subduction zone might be high enough to decompose allanite or monazite during dehydration from the subducted slab. Significant amounts of LREE could be released and concentrated in the slab-derived melts/fluids due to the decomposition, but the temperature was not high enough to decompose rutile in the subducted slab. A similar metasomatic signature was observed in the clinopyroxenes of the mantle xenoliths from several localities of Patagonia, as reported by Rivalenti *et al*. (2004a), where it was proposed that the asthenospheric mantle beneath the back-arc Patagonia region experienced a widespread partial melting, triggered by the uprising of metasomatic agents. The basaltic melts produced by such a liquid-assisted partial melting, migrated upward by a reactive porous flow through the overlying lithospheric mantle, which is therefore presently in a strongly modified form as a consequence of this interaction.

Our results indicate that the potential melts, in equilibrium with Group 2 clinopyroxenes, have geochemical patterns which are different from those of the host alkaline basalts (Fig. 9(a)). However, the patterns show marked similarities to some of the HFSE-depleted basalts (e.g., M4), which erupted in the Agua Poca region and are interpreted as being of athenospheric mantle origin affected by subduction-derived components (Bertotto *et al*., 2009). This consistency is particularly good for the highly incompatible elements, suggesting that these components in the peridotites were severely modified by interaction with the melt. Conversely, the consistency is poorer for the moderately incompatible elements, which reflect the strong depletion of the peridotites. To provide evidence for the above explanations, a Sr versus Yb diagram is shown in Fig. 9(b). Group 1 clinopyroxenes are plotted within the depletion trend of the residue, after variable degrees of partial melting (up to 6%) of a PM reservoir, while the Group 2 clinopyroxenes are plotted beyond the depletion trend. This indicates that the Group 2 clinopyroxenes are affected by slab-derived components having extremely high Sr concentrations, but the influence was more or less negligible for the Group 1 clinopyroxnes. For the reasons mentioned above, we infer that the metasomatic agent is a basaltic melt, with minor amount of slab-derived fluids.

Conceição *et al*. (2005) revealed radiogenic Sr enrichments, without a drastic change of the Nd isotopic composition, on whole rock of the lherzolite xenoliths in the whole of the Patagonian province. Such a trend on the $^{87}Sr/^{86}Sr$ vs. $^{143}Nd/^{144}Nd$ isotopic diagram, was interpreted to reflect the following three processes that took place in the mantle: i) the mixture of a depleted mantle and an enriched source (enriched mantle II - EMII); ii) the mixture of a depleted mantle and a mixture of mantle-derived and slab-derived melts; and iii) a chromatographic process that occurred during the percolation of a metasomatic agent through the mantle (Conceição *et al*., 2005). Nevertheless, major and trace element mineral chemistry of the Agua Poca spinel lherzolite do not show any clear evidence of these kinds of interactions, and they would be expected to include highly incompatible element fractionation and high concentrations (e.g., of Sr, coupled with a refractory residue) after variable degrees of melting processes. It is thus argued, that the enrichment in radiogenic Sr (as well as in other highly incompatible elements), which is exhibited by the whole rock compositions of lherzolites, is the result of a late interaction with melts and, or, fluids. Infiltration of the host basalt is locally recognized petrographically. However, the $^{87}Sr/^{86}Sr$ of the whole rock Agua Poca mantle xenoliths exceeds that of the host basalt (Jalowitzki *et al*., 2010). Thus, the occurrence of additional external fluids, and or melts, must be invoked to explain the observed whole rock Sr isotopic composition.

Acknowledgments—We thank the Facultad de Ciencias Exactas y Naturales (Universidad de La Pampa, Argentina), ANPCyT (PICT 2007-409) and CONICET (PIP 2008-358) for financial support. We appreciate the cooperation of Simona Bigi (Dipartimento di Scienze Chimiche e Geologiche, Università di Modena e Reggio Emilia, Italy) for carrying out electron microprobe analyzes, and P. Holm and M. Mazzola for their help in writing. This paper benefited from detailed and constructive reviews from T. R. Jalowitzki and two anonymous reviewers. We also give great thanks to Yuji Orihashi and Ryo Anma, for their invaluable advice with handling the editorial of the manuscript.

REFERENCES

Acevedo, R. D. and Quartino, B. J. (2004) Basalto alcalino portador de xenolitos ultramáficos en Tierra del Fuego. *Rev. Asoc. Geol. Argentina* **59**, 411–415 (in Spanish with English abstract).

Adam, J. and Green, T. (2006) Trace element partitioning between mica- and amphibole-bearing garnet lherzolite and hydrous basanitic melt: 1. Experimental results and the investigation of controls on partitioning behavior. *Contrib.*

Mineral. Petrol. **152**, 1–17.

Aliani, P. A., Bjerg, E. A. and Ntaflos, Th. (2004) Evidencias de metasomatismo en el manto sublitosférico de Patagonia. *Rev. Asoc. Geol. Argentina* **59**, 539–555 (in Spanish with English abstract).

Aliani, P. A., Ntaflos, Th. and Bjerg, E. A. (2009) Origin of melt pockets in mantle xenoliths from southern Patagonia, Argentina. *J. S. Am. Earth Sci.* **28**, 419–428.

Batanova, V. G., Suhr, G. and Sobolev, A. V. (1998) Origin of geochemical heterogeneity in the mantle peridotites from the Bay of Islands Ophiolite, Newfoundland, Canada; ion probe study of clinopyroxenes. *Geochim. Cosmochim. Acta* **62**, 853–866.

Bertotto, G. W. (2000) Cerro Agua Poca, un cono basáltico cuaternario portador de xenolitos ultramáficos, en el oeste de la provincia de La Pampa, Argentina. *Rev. Asoc. Geol. Argentina* **55**, 59–71 (in Spanish with English abstract).

Bertotto, G. W. (2002a) Xenolitos ultramáficos en el cerro De la Laguna, volcanismo basáltico de retroarco en el sureste de la provincia de Mendoza, Argentina. *Rev. Asoc. Geol. Argentina* **57**, 445–450 (in Spanish with English abstract).

Bertotto, G. W. (2002b) Cerro Huanul (37°17′ S; 68°32′ O), nueva localidad con xenolitos ultramáficos en basanitas cenozoicas del sur de Mendoza. *15th Cong. Geol. Argentino* **3**, 66–70 (in Spanish with English abstract).

Bertotto, G. W. (2003) Evolución geológica y petrológica de los conos basálticos cenozoicos portadores de xenolitos ultramáficos del margen oriental de la Provincia basáltica Andino-Cuyana, provincias de La Pampa y Mendoza. Dr. Sci. Thesis, La Plata National Univ., 196 pp. (in Spanish).

Bertotto, G. W., Cingolani, C. A. and Bjerg, E. A. (2009) Geochemical variations in Cenozoic back-arc basalts at the border of La Pampa and Mendoza provinces, Argentina. *J. S. Am. Earth Sci.* **28**, 360–373.

Bjerg, E. A., Labudía, C. H., Varela, E. and Cesaretti, N. (1994) Fluid inclusions in olivine crystals from spinel lherzolites nodules, Somuncura Massif, Argentina. *Rev. Asoc. Geol. Argentina* **50**, 257–261.

Bjerg, E. A., Kurat, G., Ntaflos, Th. and Labudía, C. H. (1999) Patagonia mantle xenoliths: petrographic, geochemical and thermobarometric data. *14th Cong. Geol. Argentino* **2**, 88.

Bjerg, E. A., Ntaflos, T., Kurat, G., Dobosi, G. and Labudía, C. H. (2005) The upper mantle beneath Patagonia, Argentina, documented by xenoliths from alkali basalts. *J. S. Am. Earth Sci.* **18**, 125–145.

Bjerg, E. A., Ntaflos, T., Thöni, M., Aliani, P. and Labudía, C. H. (2009) Heterogeneous Lithospheric Mantle beneath Northern Patagonia: Evidence from Prahuaniyeu Garnet- and Spinel-Peridotites. *J. Petrol.* **50**, 1267–1298.

Brey, G. P. and Köhler, T. (1990) Geothermobarometry in four-phase lherzolites II. New thermobarometers, and practical assessment of existing thermobarometers. *J. Petrol.* **31**, 1353–1378.

Conceição, R. V., Mallmann, G., Koester, E., Schilling, M., Bertotto, G. W. and Rodriguez-Vargas, A. (2005) Andean subduction-related mantle xenoliths: Isotopic evidence of Sr–Nd decoupling during metasomatism. *Lithos* **82**, 273–287.

Dantas, C., Greegoire, M., Koester, E., Conceição, R. V. and Rieck, N., Jr. (2009) The lherzolite–websterite xenolith suite from Northern Patagonia (Argentina): Evidence of mantle-melt reaction processes. *Lithos* **107**, 107–120.

Douglas, B. J., Saul, S. A. and Stern, C. R. (1987) Rheology of the upper mantle beneath southernmost South America inferred from peridotite xenoliths. *J. Geology* **95**, 241–253.

Gaetani, G. A. and Grove, T. L. (1998) The influence of water on melting of mantle peridotite. *Contrib. Mineral. Petrol.* **131**, 323–346.

Gelós, E. M. and Hayase, K. (1979) Estudio de las inclusiones peridotíticas en un basalto de la región de Comallo y de otras localidades de las provincias de Río Negro y Chubut. *6th Cong. Geol. Argentino* **2**, 69–82 (in Spanish with English abstract).

Gervasoni, F., Conceição, R. V., Bertotto, G. W., Gallas, M. R. and Jalowitzki, T. L. R. (2009) Experimental petrology, geochemistry and petrography of mantle xenoliths from Prahuaniyeu Volcano, Northern Patagonia, Argentine. *Geochim. Cosmochim. Acta* **72**(12), A304.

Gorring, M. L. and Kay, S. M. (2000) Carbonatite metasomatised peridotite xenoliths from southern Patagonia: implications for lithospheric processes and Neogene plateau magmatism. *Contrib. Mineral. Petrol.* **140**, 55–72.

Ionov, D. A., Bodinier, J.-L., Mukasa, S. B. and Zanetti, A. (2002) Mechanisms and sources of mantle metasomatism: Major and trace element compositions of peridotite xenoliths from spitsbergen in the context of numerical modelling. *J. Petrol.* **43**, 2219–2259.

Jalowitzki, T. L. R., Conceição, R. V., Orihashi, Y., Bertotto, G. W., Nakai, S. and Schilling, M. E. (2010) Evolução geoquímica de Peridotitos e Piroxenitos do Manto Litosférico Subcontinental do vulcão Agua Poca, Terreno Cuyania, Argentina. *Pesq. Geoc.* **37**, 143–167 (in Portuguese with English abstract).

Johnson, K. T. M., Dick, H. J. B. and Shimizu, N. (1990) Melting in oceanic upper mantle: an ion microprobe study of diopsides in abyssal peridotites. *J. Geophys. Res.* **95**, 2661–2678.

Johnston, A. D. and Stout, J. H. (1984) Development of orthopyroxene–Fe/Mg ferrite symplectites by continuous olivine oxidation. *Contrib. Mineral. Petrol.* **88**, 196–202.

Kempton, P. D., Hawkesworth, C. J., Lopez-Escobar, L., Pearson, D. G. and Ware, A. J. (1999) Spinel ± garnet lherzolite xenoliths from Pali Aike: part 2. Trace element and isotopic evidence bearing on the evolution of lithospheric mantle beneath southern Patagonia. *7th Int. Kimberlite Conf. Dawson Volume* (Gurney, J. J., Gurney, J. L., Pascoe, M. D. and Richardson, S. H., eds.), **1**, 415–428.

Kilian, R. and Stern, C. R. (2002) Constraints on the interaction between slab melts and the mantle wedge from adakitic glass in peridotite xenoliths. *Eur. J. Mineral.* **14**, 25–36.

Klimm, K., Blundy, J. D. and Green, T. H. (2008) Trace element partitioning and accessory phase saturation during H_2O-saturated melting of basalt with implications for subduction zone chemical fluxes. *J. Petrol.* **49**, 523–553.

Labudía, C. H., Bjerg, E. A. and Gregori, D. A. (1984) Nódulos de composición ultrabásica de las lavas alcalinas de la localidad de Praguaniyeu, provincia de Río Negro. *9th Cong. Geol. Argentino* **2**, 547–553 (in Spanish with English ab-

stract).

Laurora, A., Mazzucchelli, M., Rivalenti, G., Vannucci, R., Zanetti, A., Barbieri, M. A. and Cingolani, C. A. (2001) Metasomatism and melting in carbonated peridotite xenoliths from the mantle wedge: the Gobernador Gregores case (southern Patagonia). *J. Petrol.* **42**, 69–87.

Mazzucchelli, M., Zanetti, A., Rivalenti, G., Vannucci, R., Teixeira, C. C. and Tassinari, C. C. G. (2010) Age and geochemistry of mantle peridotites and diorite dykes from the Baldissero body: Insights into the Paleozoic–Mesozoic evolution of the Southern Alps. *Lithos* **119**, 485–500.

McDonough, W. F. (1990) Constraints on the composition of the continental lithospheric mantle. *Earth Planet. Sci. Lett.*, **101**, 1–18.

Mercier, J.-C. C. (1980) Single-pyroxene thermobarometry. *Tectonophysics* **70**, 1–37.

Mercier, J.-C. C. and Nicolas, A. (1975) Textures and fabrics of upper mantle peridotites as illustrated by basalts xenoliths. *J. Petrol.* **16**, 454–487.

Montecinos, P., Schärer, U., Vergara, M. and Aguirre, L. (2008) Lithospheric origin of Oligocene–Miocene magmatism in Central Chile: U–Pb ages and Sr–Pb–Hf isotope composition of minerals. *J. Petrol.* **49**, 555–580.

Muñoz, B. J. (1981) Inclusiones ultramáficas del manto superior en meseta Las Vizcachas, Última Esperanza, Magallanes, Chile. *Rev. Geol. Chile* **13–14**, 63–78.

Niemeyer, H. (1978) Nódulos máficos y ultramáficos en basaltos alcalinos de la meseta Buenos Aires, lago General Carrera, provincia de Aisén, Chile. *Rev. Asoc. Geol. Argentina* **33**, 63–75.

Nimis, P. and Grütter, H. (2010) Internally consistent geothermometers for garnet peridotites and pyroxenites. *Contrib. Mineral. Petrol.* **159**, 411–427.

Ntaflos, Th., Bjerg, E. A., Kurat, G., Hinton, R., Labudía, C. H. and Upton, B. G. J. (1999) Silicate and carbonatite melts in upper mantle xenoliths from southern Patagonia: evidence for multiple metasomatic events. *Berichte der Deutschen Mineralogischen Gesellschaft, Beihefte zum Eur. J. Mineral.* **11**, 168.

Ntaflos, Th., Bjerg, E. A., Labudía, C. H., Thöni, M., Frisicale, C. and Günther, M. (2001) Garnet-bearing xenoliths: evidence of plume activity in northern Patagonia. *Annual Goldschmidt Conf. 11th*, abstract #3126.

Ntaflos, Th., Bjerg, E. A., Labudía, C. H. and Thöni, M. (2003) Geochemical evidences for plume activity beneath Patagonian sub-continental mantle. *Geoph. Res. Abstr.* **5**, 09123.

Ntaflos, Th., Bjerg, E. A., Labudía, C. H. and Kurat, G. (2007) Depleted lithosphere from the mantle wedge beneath Tres Lagos, southern Patagonia, Argentina. *Lithos* **94**, 46–65.

Ozawa, K. (2001) Mass balance equations for open magmatic systems: Trace element behavior and its application to open system melting in the upper mantle. *J. Geophys. Res.* **106**, 13407–13434.

Ozawa, K. and Shimizu, N. (1995) Open-system melting in the upper mantle: Constraints from the Hayachine–Miyamori ophiolite, northeastern Japan. *J. Geophys. Res.* **100**, 22315–22335.

Rivalenti, G., Mazzucchelli, M., Laurora, A., Ciuffi, S., Zanetti, A., Vannucci, R. and Cingolani, C. A. (2004a) The backarc mantle lithosphere in Patagonia, South America. *J. S. Am. Earth Sci.* **17**, 121–152.

Rivalenti, G., Zanetti, A., Mazzucchelli, M., Vannucci, R. and Cingolani, C. A. (2004b) Equivocal carbonatite markers in the mantle xenoliths of the Patagonia backarc: the Gobernador Gregores case (Santa Cruz Province, Argentina). *Contrib. Mineral. Petrol.* **147**, 647–670.

Rivalenti, G., Mazzucchelli, M., Zanetti, A., Vannucci, R., Bollinger, C., Hémond, C. and Bertotto, G. W. (2007a) Xenoliths from Cerro de los Chenques (Patagonia): An example of slab-related metasomatism in the backarc lithospheric mantle. *Lithos* **99**, 45–67.

Rivalenti, G., Zanetti, A., Girardi, V. A. V., Mazzucchelli, M., Tassinari, C. C. G. and Bertotto, G. W. (2007b) The effect of the Fernando de Noronha plume on the mantle lithosphere in North-Eastern Brazil. *Lithos* **94**, 111–131.

Scambelluri, M., Vannucci, R., De Stefano, A., Preite-Martinez, M. and Rivalenti, G. (2009) CO_2 fluid and silicate glass as monitors of alkali basalt/peridotite interaction in the mantle wedge beneath Gobernador Gregores, Southern Patagonia. *Lithos* **107**, 121–133.

Schilling, M. E., Carlson, R. W., Conceição, R. V., Dantas, C., Bertotto, G. W. and Koester, E. (2008) Re–Os isotope constraints on subcontinental lithospheric mantle evolution of southern South America. *Earth Planet. Sci. Lett.* **268**, 89–101.

Skewes, M. A. and Stern, C. R. (1979) Petrology and geochemistry of alkali basalts and ultramafic inclusions from the Pali–Aike volcanic field in southern Chile and the origin of the Patagonian plateau lavas. *J. Volcanol. Geoth. Res.* **6**, 3–25.

Stern, C. R., Saul, S., Skewes, M. A. and Futa, K. (1989) Garnet peridotite xenoliths from the Pali Aike basalts of southernmost South America. *Kimberlites and Related Rocks* (Ross, J., ed.), *Geol. Soc. Australia, Spec. Publ.* **14**(2), 735–744.

Stern, C. R., Frey, F. A., Futa, K., Zartman, R. E., Peng, Z. and Kyser, K. T. (1990) Trace element and Sr, Nd, Pb, and O isotopic composition of Pliocene and Quaternary alkali basalts of the Patagonian Plateau lavas of southernmost South America. *Contrib. Mineral. Petrol.* **104**, 294–308.

Stern, C. R., Kilian, R., Olker, B., Hauri, E. H. and Kyser, T. K. (1999) Evidence from mantle xenoliths for relatively thin-100 km continental lithosphere below the Phanerozoic crust of southernmost South America. *Lithos* **48**, 217–235.

Sun, S.-S. and McDonough, W. F. (1989) Chemical and isotopic systematics of oceanic basalts; implications for mantle composition and processes. *Magmatism in the Ocean Basins* (Saunders, A. and Norry, M., eds.), *Geol. Soc. Spec. Publ.* **42**, 313–345.

Taylor, W. R. (1998) An experimental test of some geothermometer and geobarometer formulations for upper mantle peridotites with application to the thermobarometry of fertile lherzolite and garnet websterite. *Neues Jb. Min. Abh.* **172**, 381–408.

Varela, M. E., Bjerg, E. A., Clocchiatti, R., Labudía, C. H. and Kurat, G. (1997) Fluid inclusions in upper mantle xenoliths from northern Patagonia, Argentina: evidence for an upper

mantle diapir. *Mineral. Petrol.* **60**, 145–164.
Vernières, J., Godard, M. and Bodinier, J.-L. (1997) A plate model for the simulation of trace element fractionation during partial melting and magma transport in the Earth's upper mantle. *J. Geophys. Res.* **102**, 24771–24784.
Villar, L. M. (1975) Las fajas y otras manifestaciones ultrabásicas en la República Argentina y su significado metalogenético. *2nd Cong. Iberoamer. Geol. Eco.*, **3**, 135–156 (in Spanish).
Wang, J., Hattori, K. H., Kilian, R. and Stern, C. R. (2007) Metasomatism of sub-arc mantle peridotites below southernmost South America: reduction of fO_2 by slab-melt. *Contrib. Mineral. Petrol.* **153**, 607–624.
Xu, Y.-G., Menzies, M. A., Bodinier, J.-L., Bedini, R. M., Vroon, P. and Mercier, J.-C. C. (1998) Melt percolation and reaction atop a plume: evidence from the poikiloblastic peridotite xenoliths from Borée (Massif Central, France). *Contrib. Mineral. Petrol.* **132**, 65–84.

Supplementary Materials

URL (http://www.terrapub.co.jp/journals/GJ/archives/data/47/MS256.pdf)
Tables S1 to S4